Optimal Network Placement of SVC Devices

Roberto Mínguez, Federico Milano, *Member, IEEE*, Rafael Zárate-Miñano, *Student Member, IEEE*, and Antonio J. Conejo, *Fellow, IEEE*

***Abstract*—This paper addresses the optimal placement of static var compensators (SVCs) in a transmission network in such a manner that its loading margin is maximized. A multiscenario framework that includes contingencies is considered. This problem is formulated as a nonlinear programming problem that includes binary decisions, i.e., variables to decide the actual placement of the SVCs. Given the mixed-integer nonconvex nature of this problem, a Benders decomposition technique within a restart framework is used. Detailed numerical simulations on realistic electric energy systems demonstrate the appropriate behavior of the proposed technique. Conclusions are duly drawn.**

***Index Terms*—Benders decomposition, maximum loading margin, static var compensator (SVC) placement, voltage stability.**

NOMENCLATURE

Constants:

p_{D_i}	Active power demand at bus i.
q_{D_i}	Reactive power demand at bus i.

Variables:

p_{G_i}	Active power generation at bus i.
q_{G_i}	Reactive power generation at bus i.
b_{C_i}	Susceptance of an SVC at bus i.
u_i	Binary variable associated with placing an SVC at bus i.
v_i	Voltage magnitude at bus i.
θ_i	Voltage angle at bus i.
μ	Network loading margin.
ψ_k	Current magnitude through transmission line k.

Sets:

Ω_b	Set of possible static var compensator (SVC) placement buses.
Ω_G	Set of generator buses.

Numbers:

ℓ	Number of constraints involving only binary variables.
m	Number of continuous variables.
n	Number of buses and of discrete variables.
n_d	Number of SVCs.
n_{dl}	Cardinality of Ω_b, i.e., number of possible SVC locations.
n_L	Number of lines.
n_s	Number of simulations.
n_c	Number of cases including the base case and the contingencies.
p_s	Probability of case s.
p	Number of constraints involving continuous and binary variables.

Vectors and matrices are in boldface, while scalar variables are in italic (e.g., $\boldsymbol{v}$ is the vector of all voltage magnitudes $v_i; i = 1, \ldots, n$). Other symbols are defined as required in the text.

Manuscript received December 6, 2006; revised June 11, 2007. This work was supported in part by the Ministry of Science and Technology of Spain under CICYT Project DPI2006-08001 and in part by Junta de Comunidades de Castilla-La Mancha under Project PBI-05-053. Paper no. TPWRS-00861-2006.

The authors are with the University of Castilla-La Mancha, Ciudad Real 13071, Spain (e-mail: Roberto.Minguez@uclm.es; Federico.Milano@uclm.es; Rafael.Zarate@uclm.es; Antonio.Conejo@uclm.es).

Digital Object Identifier 10.1109/TPWRS.2007.907543

I. INTRODUCTION

A. Motivation and Approach

Static var compensators (SVCs) make it possible to enhance the functioning of a transmission network by increasing significantly its loading margin. Thus, SVCs are increasingly used in nowadays stressed transmission systems.

Being that the load flow equations are nonlinear, to identify in which buses SVCs should be located is a complex problem mostly treated heuristically in the available literature. Therefore, it naturally arises the need to tackle this problem in a systematic and formal way so that the best or a near-best solution is found.

This paper provides an optimization procedure based on Benders decomposition that incorporates multiple restarts for determining in which buses of a transmission network SVCs should be installed. Diverse scenarios including the base case, and contingencies are considered. The target is to maximize the loading margin. The proposed multistart Benders framework allows avoiding local minima and reaching eventually the global minimum. It should be emphasized that the methodology proposed in this paper can be straightforwardly applied to locate any type of FACTS devices. However, for the sake of clarity and simplicity, we consider only the placement of SVCs.

B. Literature Review

In the technical literature, the allocation of FACTS devices has been carried out through different strategies. In [1], a linear iterative method is proposed to find the best placement of FACTS devices in order to minimize the expected thermal generation cost and the investment cost on these devices in a hydrothermal coordination problem. In [2], a sensitivity analysis is used to locate thyristor-controlled series capacitors (TCSCs) and unified power flow controllers (UPFCs) to increase the maximum power transfer level of the system. In [3], a method based on a voltage stability index is used to find the best location of the FACTS to avoid the voltage collapse.

In [4] and [5], the FACTS location problem is solved by means of genetic algorithms to lower the cost of energy production and to improve the system loading margin, respectively. A two-step procedure is proposed in [6] to locate thyristor controlled phase shifting transformers (TCPSTs) in a system using a dc load flow model. In the first step, the system loading margin is maximized, while in the second step the total investment cost or the total number of phase shifters is minimized. In both steps a mixed-integer linear programming problem is solved. Reference [7] provides a var planning tool which considers simultaneously static constraints as well as voltage stability constraints. The formulation and implementation is based on a three-level hierarchical decomposition scheme where each subproblem is solved by the interior point method. In [8], the FACTS location problem is formulated as a mixed-integer nonlinear programming problem. The optimal placement is obtained optimizing both the investment cost in FACTS and the security in terms of the cost of operation under contingency events. The problem is considered convex and solved by Benders decomposition.

The Benders decomposition is a particularly attractive technique for the FACTS location problem because it allows treating binary and continuous variables separately, thus achieving solution efficiency for moderate computational effort. However, the Benders decomposition requires that the objective function of the considered problem, projected on the subspace of the complicating variables, has a convex hull. Unfortunately, this is not the case for the SVC allocation problem. Nevertheless, since the global minimum must lie in a convex subregion, we solve the above drawback by restarting Benders decomposition with points that cover most of the solution space and that allows searching convex subregions, which make it possible identifying local minima and eventually the global minimum. We consider this technique particularly appropriate to the SVC placement problem since the alternative is a fully heuristic search (e.g., a genetic algorithm), which generally does not allow taking into account in detail the physics of the problem.

C. Contributions

The contributions of this paper are threefold.

1) A novel technique: A Benders decomposition technique incorporating multiple restarts is used to place SVCs in a transmission network. This technique allows tackling nonconvexities.
2) An efficacious and robust algorithm: The proposed decomposition is efficacious in locating globally optimal or near-optimal solutions and robust in what refers to computational behavior.
3) A proven procedure: Detailed numerical simulations considering different realistic electric energy systems prove the good behavior of the proposed technique.

D. Paper Organization

The rest of this paper is organized as follows. Section II provides the detailed formulation of the considered problem. In Section III the proposed solution algorithm is stated. Section IV provides and analyzes results for a 40-bus system, and two realistic systems, namely, the IEEE 300-bus test system and a 1228-bus Italian network. Section V gives some relevant conclusions.

II. Formulation

In this paper, the following mixed-integer nonlinear programming problem is used to compute the maximum loading condition of a network

$$\underset{\boldsymbol{u},\mu,\boldsymbol{v},\boldsymbol{\theta},\boldsymbol{p}_G,\boldsymbol{q}_G,\boldsymbol{b}_C,\boldsymbol{\psi}}{\text{Minimize}} \quad z=-\mu \tag{1}$$

$$\text{subject to}$$

$$0=p_{G_i}-\mu p_{D_i} - \sum_{j=1}^{n}(v_i v_j B_{ij}\sin(\theta_i-\theta_j)+v_i v_j G_{ij}\cos(\theta_i-\theta_j)); \quad i=1,\ldots,n, \tag{2}$$

$$0=q_{G_i}-\mu q_{D_i}+b_{C_i}v_i^2 - \sum_{j=1}^{n}(v_i v_j G_{ij}\sin(\theta_i-\theta_j)-v_i v_j B_{ij}\cos(\theta_i-\theta_j)); \quad i=1,\ldots,n, \tag{3}$$

$$\psi_k^{\max}\geq\left|j\frac{b_{k0}}{2}v_i e^{j\theta_i}+(g_k+jb_k)(v_i e^{j\theta_i}-v_j e^{j\theta_j})\right| \quad k=(i,j)=1,\ldots,n_L, \tag{4}$$

$$0=u_i;\quad \forall i\in\Omega_G, \tag{5}$$

$$0=\theta_{\text{ref}}, \tag{6}$$

and

$$p_{G_i}^{\min}\leq p_{G_i}\leq p_{G_i}^{\max}\qquad \forall i=1,\ldots,n \tag{7}$$

$$q_{G_i}^{\min}\leq q_{G_i}\leq q_{G_i}^{\max}\qquad \forall i=1,\ldots,n \tag{8}$$

$$v_i^{\min}\leq v_i\leq v_i^{\max}\qquad \forall i=1,\ldots,n \tag{9}$$

$$-\pi\leq\theta_i\leq\pi\qquad \forall i=1,\ldots,n \tag{10}$$

$$u_i b_{C_i}^{\min}\leq b_{C_i}\leq u_i b_{C_i}^{\max}\qquad \forall i=1,\ldots,n \tag{11}$$

$$\sum_{i}^{n}u_i\leq n_d \tag{12}$$

where the notation of most variables, constants, and numbers is given at the beginning of this paper and $G_{ij}+jB_{ij}$ are the elements of the admittance matrix of the network, and g_k+jb_k and b_{k0} are the series admittance and the shunt susceptance, respectively, of the transmission line k. The discrete variables $\boldsymbol{u}\in\{0,1\}^n$ define the placement of the SVCs, i.e., if $u_i=1$, an SVC is placed at bus i.

The objective function and the equality and inequality constraints in (1)–(12) are explained below.

A. Objective Function

Minimizing $-\mu$ corresponds to find the maximum loading condition that can be associated with either [9]

1) voltage stability limit (collapse point) corresponding to a system singularity (saddle-node bifurcation);
2) system controller limits such as generator reactive power limits (limit-induced bifurcation);
3) thermal or bus voltage limit.

Observe that (1) is the simplest objective function that allows taking into account voltage stability constraints [10]. Other more sophisticated models have been proposed in [11] and [12]. Nevertheless, the main goal of this paper is to formulate the maximum loading condition problem as a mixed-integer nonlinear programming problem and solve it by means of a robust technique. Thus, the conclusions to be drawn using (1) can be extended to other objective functions and OPF models of the form (1)–(12).

B. Equality Constraints

The system functioning is represented by the power flow (2) and (3), and the current flows in transmission lines and transformers (4). According to typical assumptions in voltage stability studies [9], the loading margin μ is a scalar value that increases uniformly the active and reactive powers of all loads. Thus, the power factor of load powers is assumed to be constant. Equation (5) imposes that the SVCs cannot be installed at generator buses, as it is common practice. Finally (6) is needed to fix the reference bus phase angle.

For simplicity, it is assumed that there is at most one generator (p_{G_i}, q_{G_i}) at each bus. If no generator is connected at bus i, then

$$p_{G_i}^{\max} = p_{G_i}^{\min} = 0, \quad q_{G_i}^{\max} = q_{G_i}^{\min} = 0. \tag{13}$$

For the sake of simplicity, but without lack of generality, SVC devices are modeled as variable susceptances. More sophisticated models (e.g., the fundamental frequency firing angle model) can be implemented but doing so does not change the solution technique that is proposed in this paper. It should also be noted that different steady-state models of FACTS, i.e., TCSCs, UPFCs, TCPSRs, etc., can be straightforwardly incorporated in problems (1)–(12).

C. Inequality Constraints

The physical and security limits considered in this paper are similar to those proposed in [13], and take into account generator active (7) and reactive limits (8), voltage magnitude limits (9), and transmission line thermal limits (4). Inequalities (10) are used for limiting voltage angles, eventually improving the convergence of the optimization method. Inequalities (11) are used for limiting the susceptance of installed SVCs; if the SVC is not placed at the bus i, the associated SVC susceptance limits are set to zero. Finally, (12) imposes that the maximum number of installed SVCs is n_d.

III. Solution

A. Compact Formulation

The SVC placement problem formulated in Section II can be expanded to consider multiple scenarios (base case and contingencies) and reformulated in a compact manner as

$$\underset{\boldsymbol{u},\boldsymbol{x}}{\text{minimize}} \quad z = \sum_{s=1}^{n_c} p_s f_s(\boldsymbol{u}, \boldsymbol{x}_s) \tag{14}$$

$$\text{subject to}$$

$$\boldsymbol{h}_s(\boldsymbol{u}, \boldsymbol{x}_s) \le \boldsymbol{0}; s = 1, \ldots, n_c \tag{15}$$

$$\boldsymbol{g}_s(\boldsymbol{u}) \le \boldsymbol{0}; s = 1, \ldots, n_c \tag{16}$$

where $\boldsymbol{u} \in \{0,1\}^n, \boldsymbol{x}_s \in \mathbb{R}^m, f_s(\boldsymbol{u}, \boldsymbol{x}_s) : \{0,1\}^n \times \mathbb{R}^m \to \mathbb{R}, \boldsymbol{h}_s(\boldsymbol{u}, \boldsymbol{x}_s) : \{0,1\}^n \times \mathbb{R}^m \to \mathbb{R}^p$, and $\boldsymbol{g}(\boldsymbol{u}) : \{0,1\}^n \to \mathbb{R}^\ell$, and constraints (15) and (16) include both equality and inequality constraints. Note that $\sum_{s=1}^{n_c} p_s = 1$. Note also that s refers to different scenarios (i.e., base case and contingencies) and p_s is the probability associated with the occurrence of scenario s. It should be noted that the above formulation considers simultaneously one base case scenario and several contingency scenarios. Observe also that SVC placement variables $\boldsymbol{u}$ do not depend on the scenario while operational variables $\boldsymbol{x}_s$ do.

Note that the objective function (14) provides a measure of the average impact on system security (average loading margin) resulting from the availability of SVCs. This average value is computed for all plausible loading and contingency scenarios properly weighted by their corresponding probabilities of occurrence.

B. Solution Algorithm

The proposed multistart Benders decomposition procedure for problems (14)–(16) shown in Fig. 1 works as follows [14].

1) *Global Initialization*. Set the simulation counter to $j = 0$ and $z^{\text{opt}} = \infty$, where z^{opt} is the global minimum of problems (14)–(16).
2) *Random Initial Solution*. Place randomly the available SVCs in the network, i.e., initialize $\boldsymbol{u}_0$, and update the simulation counter $j \leftarrow j + 1$.
3) *Benders Initialization*. Set the Benders iteration counter to $\nu = 1, \boldsymbol{u}^{(\nu)} = \boldsymbol{u}_0$, and $z_{\text{down}}^{(\nu)} = -\infty$.
   Note that the lower bound of the objective function optimal value is initialized to $-\infty$.
4) *Subproblem Solutions*. Solve for all cases considered $s = 1, \ldots, n_c$ (base case and contingencies)

$$\underset{\boldsymbol{x}_s}{\text{minimize}} \quad z = f_s(\boldsymbol{u}, \boldsymbol{x}_s) \tag{17}$$

$$\text{subject to}$$

$$\boldsymbol{h}_s(\boldsymbol{u}, \boldsymbol{x}_s) \le \boldsymbol{0} \tag{18}$$

$$\boldsymbol{u} = \boldsymbol{u}^{(\nu)} : \quad \boldsymbol{\lambda}_s^{(\nu)}. \tag{19}$$

The solution of this subproblem provides ${\boldsymbol{x}_s}^{(\nu)}, f_s(\boldsymbol{u}^{(\nu)}, {\boldsymbol{x}_s}^{(\nu)})$ and $\boldsymbol{\lambda}_s^{(\nu)}$. It should be noted that $\boldsymbol{\lambda}_s^{(\nu)}$ is the dual variable associated with (19).

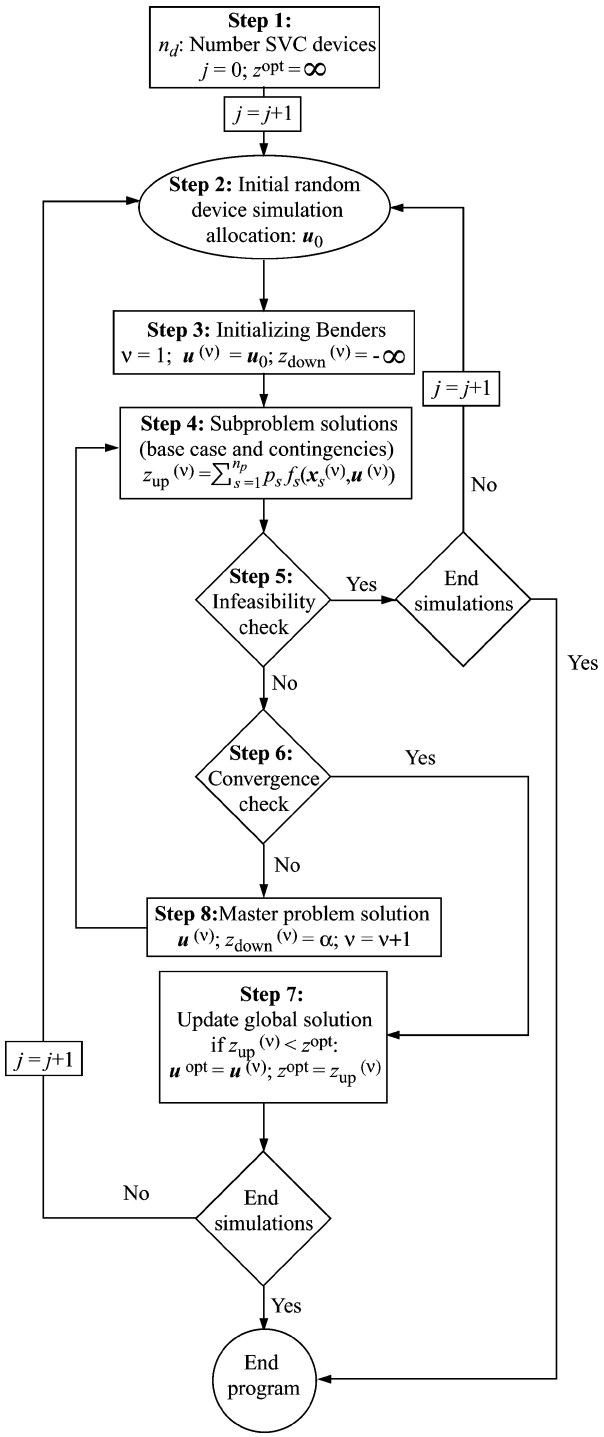

Fig. 1. Structure of the proposed multistart Benders framework.

Update the objective function upper bound, $z_{\rm up}^{(\nu)} = \sum_{s=1}^{n_c} p_s f_s(\boldsymbol{u}^{(\nu)}, \boldsymbol{x}_s^{(\nu)})$.

Note that since $\boldsymbol{u}^{(\nu)}$ is not generally optimal, $z_{\rm up}^{(\nu)}$ constitutes an upper bound of the objective function optimal value.

Observe that (1)–(12) corresponds to one instance of problem (17)–(19) once variables $\boldsymbol{u}$ are fixed to trial values. An interesting feature of the Benders decomposition technique is that the n_c problems (17)–(19), corresponding to the base case and the contingencies, are decoupled and can thus be solved in parallel.

5) *Infeasibility Check*. If $z_{\rm up}^{(\nu)} < z_{\rm down}^{(\nu)}$ or $\nu = \nu_{\max}$ a nonconvex region is wrongly reconstructed and no solution can be identified; if the number of prespecified rounds (n_s) has not been reached go to 2), otherwise the algorithm concludes. In any other case the algorithm continues below.
6) *Convergence Check*. If $|z_{\rm up}^{(\nu)} - z_{\rm down}^{(\nu)}|/|z_{\rm down}^{(\nu)}| \le \varepsilon$, a solution with a level of accuracy ε has been found

$$\boldsymbol{u}^* = \boldsymbol{u}^{(\nu)}$$

and the algorithm continues below; otherwise, it continuous in 8).
7) *Global Solution Update*. If $z_{\rm up}^{(\nu)} < z^{\rm opt}$ update the global solution $z^{\rm opt} = z_{\rm up}^{(\nu)}, \boldsymbol{u}^{\rm opt} = \boldsymbol{u}^*$ and the algorithm continues in 2) if the number of prespecified rounds has not been reached; otherwise, the algorithm concludes. In any other case, the algorithm continues below.
8) *Master Problem Solution*. Update the iteration counter $\nu \leftarrow \nu + 1$ and solve

$$\underset{\alpha, \boldsymbol{u}}{\text{minimize}} \quad \alpha \tag{20}$$

$$\text{subject to}$$

$$\boldsymbol{g}_s(\boldsymbol{u}) \le \boldsymbol{0}; s = 1, \ldots, n_c. \tag{21}$$

$$\alpha \ge \sum_{s=1}^{n_c} p_s f_s(\boldsymbol{u}^{(i)}, \boldsymbol{x}_s^{(i)}) + \sum_{s=1}^{n_c} \sum_{k=1}^{n} \lambda_{sk}^{(i)} \left(u_k - u_k^{(i)}\right); \quad i = 1, \ldots, \nu - 1 \tag{22}$$

$$\alpha \le z^{\rm opt}. \tag{23}$$

Note that at each iteration one additional constraint (22) is added to problem (20)–(23). Constraint (23) forces to look for solutions with objective function value lower than or equal to the current optimum $z^{\rm opt}$ thus seeking better and better solutions. Note that (23) increases the failure rate of the Benders scheme but ensures that solutions found are successively better and better. The solution of this master problem provides $\boldsymbol{u}^{(\nu)}$ and $\alpha^{(\nu)}$.

Update the objective function lower bound $z_{\rm down}^{(\nu)} = \alpha^{(\nu)}$.

The algorithm continues in 4).

It should be noted that problem (20)–(23) approximates successively problems (14)–(16). Note that $\alpha^{(\nu)}$ constitutes a lower bound of the optimal value of the objective function because problems (20)–(23) approximates from below problem (14)–(16). If the Benders decomposition technique converges, then, $\alpha^{(\nu)} = z^{(\nu)}$.

C. Generation of Initial Solutions

A relevant issue concerning the performance of the proposed method is how to generate random initial SVC allocations in order to restart the Benders procedure. It should be noted that the SVC locations are randomly generated just as starting points

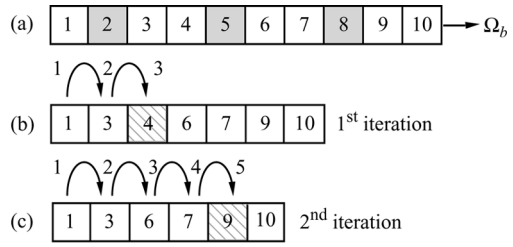

Fig. 2. Simulation procedure for a 10-bus system.

for the Benders algorithm and with the purpose of exploring the whole feasibility region so that the global maximum is not missing.

Let us consider a 10-bus system with 3 generation buses corresponding to buses 2, 5, and 8, respectively, as indicated in Fig. 2(a) using gray shadows. The aim is to generate an initial random positioning for $n_d = 6$ SVCs. As no device can be located at generation buses, for the first iteration set Ω_b with n_d components is initialized including just the positions where SVCs can be located as shown in Fig. 2(a). Next, a random integer value between 1 and the cardinality of $\Omega_b(n_{dl} = 7)$ is generated using "$\mathrm{round}(\mathrm{uniform}(0.5, n_{dl}{+}0.5))$," where a uniformly random number between 0.5 and $n_{dl}+0.5$ is rounded to the nearest integer. Note that using this expression, the probability of obtaining any of the integers on the list is equally likely. Considering that a 3 has been obtained, the first device is located at the position indicated by the third component of set Ω_b, i.e., bus 4 [see Fig. 2(b)]. For the next iteration, set Ω_b is updated because no additional SVCs can be installed in bus 4. The cardinality of Ω_b is updated $n_{dl} = n_{dl} - 1 = 6$, and a random integer value is obtained using the same expression. Considering the resulting random integer number to be 5, the second SVC is located at the position indicated by the fifth component of set Ω_b, i.e., bus 9 [see Fig. 2(c)]. The procedure continues until all SVCs have been placed.

Note that this procedure allows us to randomly generate a feasible initial solution for the Benders decomposition procedure with a probability of occurrence of

$$\binom{n_{dl}}{n_d}^{-1} = \frac{n_d!}{n_{dl}(n_{dl}-1)(n_{dl}-2)\cdots(n_{dl}-n_d+1)}. \tag{24}$$

In general, the algorithm to generate initial solutions proceeds as stated in the following.

1) Data and initialization: Required data include the set of possible device locations Ω_b, its cardinality n_{dl} and the number of SVCs to be installed n_d.
   Set the iteration counter to $\nu = 1$, and all the components of $\boldsymbol{u}_0$ to zero.
2) Random number generation: Obtain the first random integer number r_n using the expression

$$r_n = \mathrm{round}(\mathrm{uniform}(0.5, n_{dl} + 0.5)). \tag{25}$$

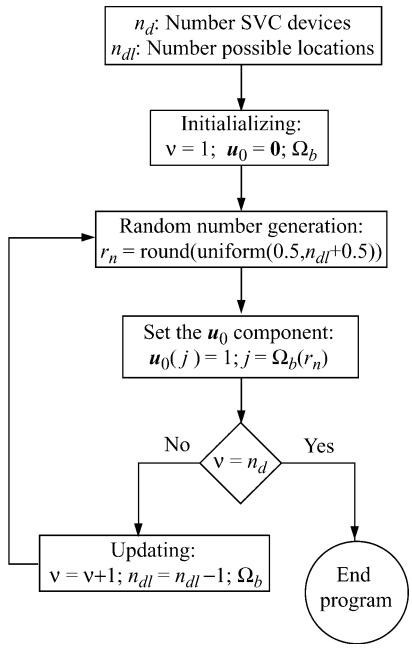

Fig. 3. Flow chart of the algorithm to generate random initial solutions.

3) SVC placement: Set the jth component in vector $\boldsymbol{u}_0$ corresponding to the r_nth element in set Ω_b to 1.
4) Stopping criterion: If $\nu = n_d$ the procedure concludes, otherwise update the iteration counter $\nu = \nu + 1$, the set Ω_b and the remaining number of possible device locations $n_{dl} = n_{dl} - 1$, and continue in 2).

The flow chart of the algorithm to generate random initial solutions is shown in Fig. 3.

IV. Case Studies

A. Southwest England 40-Bus System

This section discusses a case study based on the 40-bus test system shown in Fig. 4. This system is based on a simplified model of the Southwest England power system and firstly appeared in [15]. Most power flow data can be found in [16] while the system limits used in this paper are provided in the Appendix. The network includes 40 buses, 65 lines, and 17 loads for a total base-case load of 41 MW and 7 Mvar. There are three voltage levels, namely 132, 33, and 11 kV. A feeding substation is located at bus 40 at 132 kV. Buses 20, 22, and 29-37 are at 11 kV, while all remaining buses are at 33 kV. Generators are located at buses 6, 13, 18, 20, 22, 24, and 39.

The original network does not contain SVCs. In this case, compensation is obtained through a static condenser at bus 12 and proper values of tap ratios of 33/11 kV transformers. These are the transformers that connect buses 1–29, 2–30, 3–31, 4–31, 5–32, 8–36, 9–35, 10–33, 11–34, 27–37, and 28–37, respectively. For the sake of simplicity, we assume that the tap ratios of these transformers are fixed.

The maximum number of SVCs that can be allocated in this system is 33, i.e., the number of buses minus the number of generators (no SVC is located at generator buses).

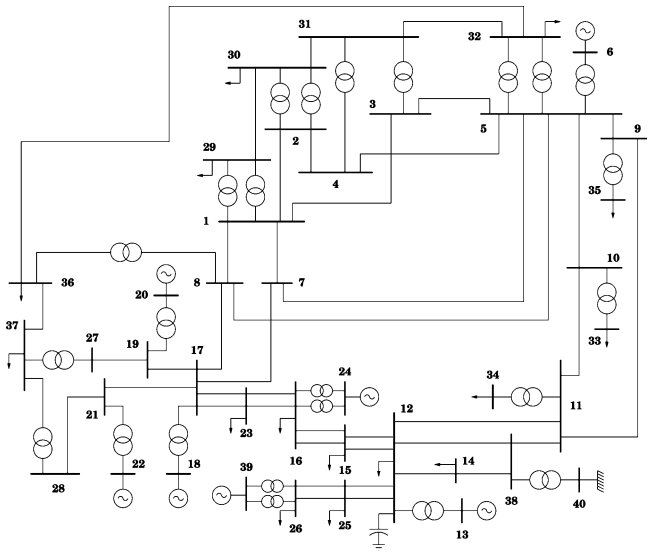

Fig. 4. The 40-bus test system.

In the simulations, we consider the base case scenario and the four "worst case" contingencies corresponding to the outages of the lines 29–1, 26–39, 17–18, and 5–6, respectively. Contingency scenarios are sorted in increasing order of potential damage. Furthermore, we also study a multiscenario model where the objective function (14) is the average loading margin for the different cases multiplied by their corresponding probabilities of occurrence, i.e.,

$$z = -\sum_{s=1}^{n_c} p_s \mu_s \tag{26}$$

where the p_s-values for this example are $p_1 = 80\%$ for the base case, and $p_2 = 8\%, p_3 = 4\%, p_4 = 4\%$, and $p_5 = 4\%$ for the line outage cases, respectively.

Up to 5 SVCs (i.e., $n_d \in [1, 5]$) and 200 different initial solutions for each number of SVCs have been considered for each scenario. Observe that for $n_d = 1$, it is sufficient to place the SVC at each bus and then to check which placement provides the maximum loading margin. However, the case $n_d = 1$ is included for the sake of completeness. The optimization problems are solved using CPLEX 10.0 (master problem) and MINOS 5.51 (subproblems) under GAMS [17] with a Sun Fire V20Z with 2 processors at 2.40 GHz and 8 GB of RAM memory.

Table I provides the results for each scenario and for each value of n_d. The first column shows the maximum loading margin without SVC placement (μ_0)) and the percentage of times the Benders procedure fails to converge $(\mathrm{NC}_{\%})$ for the first 200×5 runs (5 cases considering from 1 to 5 SVCs and 200 simulations for each case). The loading margin μ provided in the third column of Table I is the maximum value obtained after the 200 simulations. The fourth column provides the number of times that the Benders procedure converges to the global optimal solution using different initial solutions. The SVC placement depicted in the fifth column corresponds to the maximum value of the loading margin μ. The last column of Table I shows the CPU time in seconds needed to complete the 200 simulations for each scenario. Observe that the number

TABLE I
MAXIMUM LOADING MARGIN AND SVC LOCATIONS FOR DIFFERENT SCENARIOS FOR THE 40-BUS TEST SYSTEM

Case	n_d	μ	Freq.	Positions	CPU(s)
Base case	1	1.991	55	29	21.69
$\mu_0 = 1.865$	2	2.092	73	29,30	31.87
$\mathrm{NC}_{\%} = 84.85$	3	2.191	10	29,30,32	59.28
	4	2.290	6	29,30,31,32	79.27
	5	2.369	4	28,29,30,31,32	117.53
Contingency 1	1	1.267	182	29	95.03
$\mu_0 = 0.637$	2	1.411	200	29,30	116.58
$\mathrm{NC}_{\%} = 44.7$	3	1.431	28	29,30,31	336.06
	4	1.444	11	2,29,30,31	432.26
	5	1.450	10	1,2,29,30,33	637.29
Contingency 2	1	1.534	183	26	26.75
$\mu_0 = 1.471$	2	1.576	200	25,26	39.39
$\mathrm{NC}_{\%} = 53.15$	3	1.592	198	12,25,26	96.22
	4	1.610	196	12,25,26,33	152.75
	5	1.630	193	12,15,25,26,33	198.83
Contingency 3	1	1.759	11	29	20.70
$\mu_0 = 1.640$	2	1.848	130	29,30	27.5
$\mathrm{NC}_{\%} = 86.78$	3	1.939	21	29,30,36	50.31
	4	2.026	5	29,30,32,37	95.24
	5	2.096	2	27,28,29,30,32	164.61
Contingency 4	1	1.839	60	29	17.97
$\mu_0 = 1.720$	2	1.932	75	29,30	27.40
$\mathrm{NC}_{\%} = 83.5$	3	2.021	18	29,30,32	56.11
	4	2.087	1	28,29,30,32	83.16
	5	2.145	19	1,2,19,30,31	148.68
Multi-scenario case	1	1.897	29	29	1597.84
$\mu_0 = 1.736$	2	1.997	131	29,30	1696.54
$\mathrm{NC}_{\%} = 91.6$	3	2.084	114	29,30,32	3463.68
	4	2.170	2	28,29,30,32	4320.69
	5	2.226	1	1,2,19,30,31	6269.62

μ_0: Maximum loading margin without SVC.
$\mathrm{NC}_{\%}$: Percentage of convergence failures.

of SVCs located is always equal to n_d, although (12) only imposes that the number of SVCs is smaller than or equal to n_d. This result is to be expected since the higher the number of SVCs installed in the network, the higher the loadability of the network.

It is relevant to note that for the outage of line 29–1 (contingency 1), the solution without SVCs is not feasible, in fact $\mu_0 = 0.637 < 1$. After the SVC placement, the system complies the N-1 security criterion, i.e., $\mu > 1$ for $n_d \geq 1$.

Note that for the multiscenario case, the result up to 3 SVCs is equal to the results for the base case and the contingency case 4, while for 4 and 5 SVCs the result of the multiscenario case is the same as that of contingency case 4.

Fig. 5 illustrates the loading margin μ as a function of the number of installed SVCs, n_d. For the sake of illustration, in this case up to 20 SVCs (i.e., $n_d \in [1, 20]$) have been considered. The black dots indicate the best values of μ found, while light gray dots indicate the values of μ obtained with suboptimal SVC placements. Fig. 5(a) depicts the solution for the base case and for each contingency considered separately. As expected, the base case leads to the highest loading margins. Observe that the optimal value of μ saturates below 20 SVCs for contingencies 1 and 2. This result is to be expected, since the maximum loading condition is given by the transmission line

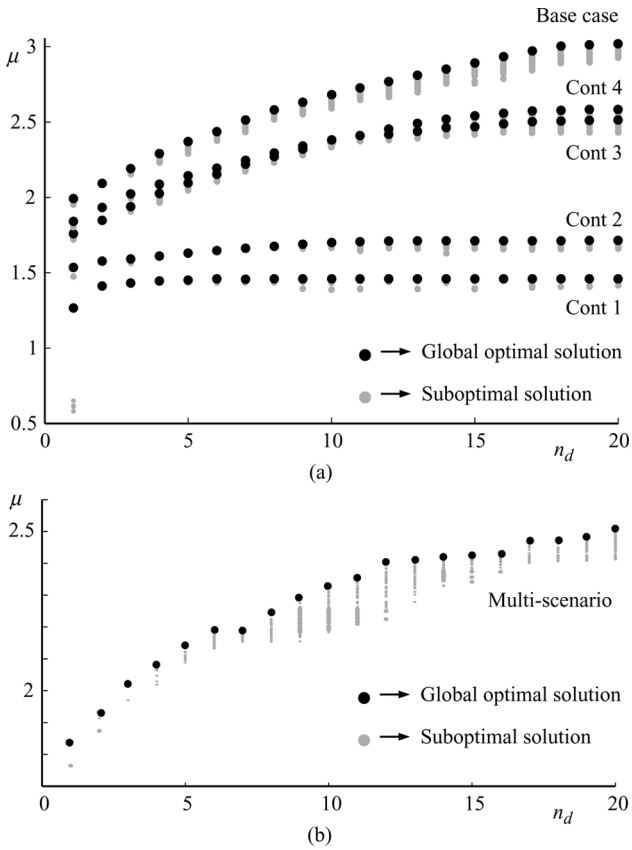

Fig. 5. Evolution of the loading margin μ as a function of the number of installed SVCs n_d for the different cases. (a) Separate solutions for the base case and each contingency. (b) Solution of the multiscenario model that includes the base case and all contingencies.

thermal limits or by the saddle-node bifurcation if there is no reactive power problem. Fig. 5(b) depicts the solution of the multiscenario problem that includes a weighted average of the base case and the 4 worst contingencies. Observe that the low probability of the contingencies with respect to the base case leads to high values of the loading margin μ. Simulation results considering the 20 cases show that the percent of variation, which is equal to the difference between the maximum and the minimum obtained loading margins divided by the average value $(\overline{\mu})$, is between 0 and 4% for all cases. The percentage of times the Benders decomposition fails to converge varies between 0 and 98% across the cases considered. The simulation number where the maximum loading margin is obtained ranges from 1 to 194.

For the sake of comparison, Table II provides the ten smallest eigenvalues of the reduced power flow Jacobian matrix of the 40-bus system obtained using the well-known QV sensitivity approach proposed in [18]. The Jacobian matrix is computed for the base case loading condition.

According to the QV sensitivity analysis, the buses associated through participation factors with the lowest eigenvalues are the best candidates for reactive power compensation. The weakest bus is bus 29, which is also the bus provided in Table I for $n_d = 1$. However, as the maximum number of device n_d increases, the sensitivity analysis is only able to provide rough information on the best bus candidates for the placement of SVC devices. For example, for $n_d = 2$, the optimal solution in Table I

TABLE II
QV SENSITIVITY ANALYSIS FOR THE 40-BUS TEST SYSTEM

JME	Most Related Bus	JME	Most Related Bus
0.06915	29	0.32905	27
0.16723	37	0.35115	34
0.19875	33	0.37380	34
0.23486	35	0.50884	30
0.30984	29	0.56537	2

JME: Jacobian Matrix Eigenvalue.

TABLE III
COMPARISON BETWEEN BENDERS DECOMPOSITION AND QV SENSITIVITY ANALYSIS FOR THE 40-BUS TEST SYSTEM

	Benders Decomposition		QV Sensitivity Analysis	
n_d	Bus #	μ	Bus #	μ
1	29	1.991	29	1.991
2	29, 30	2.092	29, 37	2.088
3	29, 30, 32	2.191	29, 33, 37	2.129
4	29, 30, 31, 32	2.290	29, 33, 35, 37	2.209
5	28, 29, 30, 31, 32	2.369	27, 29, 33, 35, 37	2.283

TABLE IV
COMPARISON BETWEEN MULTISTART BENDERS DECOMPOSITION AND STANDARD BENDERS DECOMPOSITION FOR THE 40-BUS TEST SYSTEM

	Multi-start Benders Decomposition		Standard Benders	
n_d	Bus #	μ	Bus #	μ
1	29	1.991	7	1.951
2	29, 30	2.092	29, 30	2.092
3	29, 30, 32	2.191	29, 30, 32	2.191
4	29, 30, 31, 32	2.290	29, 30, 31, 32	2.290
5	28, 29, 30, 31, 32	2.369	2, 29, 30, 31, 32	2.353

for the base case provides buses 29 and 30. On the other hand, the sensitivity analysis is only able to show that buses 29 and 30 are among the 10 weakest buses of the system. Table III shows a comparison of the maximum loading margins μ obtained using the proposed Benders decomposition technique and the QV sensitivity analysis method. Observe that the Benders decomposition technique is able to find better SVC placement solutions for $n_d > 1$.

It should also be noted that if a standard Benders procedure is used [14] (with no restart), the solution attained is generally worse than the one obtained by the proposed multistart Benders algorithm. Table IV compares the solutions of both methods.

B. IEEE 300-Bus Test System

This section presents and discusses a case study based on the IEEE 300-bus test system [19]. The aim of this case study is to show that the proposed Benders decomposition technique is feasible for large networks. Due to space limitations, only the base case is considered in this case study.

The maximum number of SVCs that can be allocated in this system is 231, i.e., the number of buses minus the number of generators.

For this case study, we consider up to 5 SVCs (i.e., $n_d \in [1, 5]$), and 500 different initial solutions for each value n_d of SVCs.

TABLE V
OPTIMAL LOADING MARGIN AND SVC LOCATIONS FOR THE IEEE 300-BUS SYSTEM

Case	n_d	μ	Freq.	Positions	CPU(s)
Base case	1	1.079	120	154	16395.43
$\mu_0 = 1.068$	2	1.128	1	105,124	19614.56
$\mathrm{NC}_{\%} = 68.4$	3	1.147	8	124,136,270	39129.58
	4	1.192	2	96,124,130, 270	45958.82
	5	1.207	5	97, 111, 152, 159, 270	72836.48

μ_0: Maximum loading margin without SVC.
$\mathrm{NC}_{\%}$: Percentage of convergence failures.

Results for the IEEE 300-bus test system are given in Table V, which provides similar information as Table I but for the IEEE 300-bus system.

Table VI provides simulation results up to 5 SVCs, where $\bar{\mu}$ is the loading margin mean value for the 500 simulations, σ is the loading margin standard deviation, range is the difference between the maximum and the minimum loading margins obtained, "% of variation" is equal to the range divided by the average value ($\bar{\mu}$), "% of failure" is the percentage of times the Benders decomposition fails to converge, n_{sim} is the simulation number corresponding to the maximum loading margin, n_{dif} is the number of different solutions obtained by means of the Benders decomposition, and n_{sol} is the number of different possible SVC placement configurations obtained through the inverse of formula (24).

Note that the solution for more than one SVC does not include the optimal position for 1 SVC, showing that the QV sensitivity analysis method fails to obtain the global optimum if the number of SVC is greater than 1.

The most likely global optima for the placement of 1 to 5 SVCs are obtained at iterations 169, 466, 186, 243, and 87, respectively (see Table VI). Note that in most cases the optimum is obtained in fewer iterations than 500 (number of restarts).

C. 1228-Bus Italian Network

For the sake of completeness the proposed method is applied to a real-world 1228-bus model of the Italian transmission grid. Due to space limitations only the base case is considered.

For this case study, we consider up to 3 SVCs and 200 different initial solutions for each value n_d of SVCs.

Results are given in Table VII, which provides similar information as Table I. Table VII also provides information about the first solution of the method, corresponding to the standard Benders approach. The following observations are pertinent.

1) The solution provided by the multistart Benders method is better than the one provided by the sensitivity based technique. Note that the three nodes associated with the weakest eigenvalues of the Jacobian matrix are 483, 758 and 413, respectively. The objective function values corresponding to the positioning of one SVC at node 483, two SVCs at nodes 483 and 758, and three SVCs at nodes 483, 758 and 413, are $\mu_1 = 1.8752, \mu_2 = 1.8755$ and $\mu_3 = 1.8788$, respectively, which are worse solutions than those provided by the proposed technique (see Table VII).
2) Even if the Benders decomposition method with only one starting point is considered (standard Benders), results are better than those obtained using the sensitivity method.
3) For 2 SVCs, there are two equivalent solutions because the corresponding objective functions are almost the same and nodes 241 and 242 are geographically very close. Since this is the only solution obtained through the simulation process, we can affirm with a high confidence level that this is the global optimum.
4) For the case of three SVCs, only two different solutions are obtained through the simulation process. Note that the optimal solution corresponds to nodes 240, 241, and 242.

Buses 483 and 413 are located in Northeast Italy, while bus 758 is in the South. These buses belong to scarcely interconnected subtransmission networks at 132 kV. Hence, these buses present high participation factors with respect to the lowest eigenvalues of the power flow Jacobian matrix. Although placing SVC devices at these buses can locally improve voltage levels, this does not necessarily implies a benefit for the whole Italian grid.

Buses 313, 240, 241, and 242 are well interconnected 400 kV buses located in the North of Italy, in between Switzerland and the industrial area of Milan. These buses are not particularly weak since they are well interconnected to the HV network. However, a voltage support of the heavily loaded area of Milan improve the loading margin of the whole Italian grid. Observe also that to place several SVCs at buses geographically close basically means that the requirement of reactive power of the area of Milan is higher than the maximum capacity of a single SVC. This information cannot be deduced from the sensitivity analysis.

Finally, note that the computing time needed by the sensitivity technique is basically the time required to compute the eigenvalues of the corresponding power flow Jacobian matrix. This time is generally much smaller than the computing time required by the proposed Benders procedure. For example, to locate 3 SVCs in the 1228-bus Italian network, the time required by the sensitivity technique is 10 seconds (that is, the CPU time needed to compute the 3 smallest eigenvalues of the power flow Jacobian matrix and the associated bus participation factors) whereas the time required by the Benders technique considering 200 restarts is about 52 h.

D. Remarks

From the results obtained in the case studies, the following observations are pertinent.

1) The maximum loading margin saturates as the number of SVC devices increases under two different situations: a) the maximum loading condition is imposed by transmission line thermal limits or b) a saddle-node bifurcation occurs if there is no reactive power shortage. For both cases adding new SVCs does not improve significantly the loading margin.
2) Differences in μ range up to 7%. This fact can be useful in case that a suboptimal solution is more acceptable than the optimal one for practical reasons (e.g., reachability of the bus, availability of the area around the bus for the installation of the SVC, etc.).

TABLE VI
RESULTS UP TO 5 SVCS FOR THE IEEE 300-BUS SYSTEM

n_d	μ	$\bar{\mu}$	σ	range	% variation	% failure	n_{sim}	n_{dif}	n_{sol}
1	1.079	1.078	0.00395	0.01190	1.10379	70.20	169	4	231
2	1.129	1.128	0.00527	0.06129	5.43239	20.20	466	5	26565
3	1.147	1.143	0.00699	0.07946	6.95149	66.00	186	9	2027795
4	1.192	1.171	0.04576	0.12433	10.61796	91.00	243	4	115584315
5	1.207	1.173	0.05930	0.13977	11.91395	94.60	87	3	5247527901

TABLE VII
OPTIMAL LOADING MARGIN AND SVC LOCATIONS FOR THE 1228-BUS ITALIAN SYSTEM

Case	n_d	μ	Freq.	Positions	CPU(s)
Base case	1	1.8846*	30	240	463.55
$\mu_0 = 1.8716$		1.8847	1	313	92710.35
$\text{NC}_{\%} = 88.2$	2	1.8975*	5	240,241	819.51
		1.8975	10	240,241 or 242	163902.57
	3	1.9090*	1	240,242,358	935.82
		1.9104	28	240,241,242	187163.98

μ_0: Maximum loading margin without SVC.
$\text{NC}_{\%}$: Percentage of convergence failures.
$*$: Standard Benders solution.

3) The number of times that the Benders procedure fails to converge, ranging from 0% to 98%, and the number of repetitions of the different solutions obtained show both the globally nonconvex character of the problem and the existence of local convex regions.
4) Simulations point out the existence of clearly different local minima.
5) The number of occurrences of the globally optimal solution varies considerably with the number of SVCs to be installed.
6) For the considered case-studies, the proposed method performs better than the sensitivity method. For the base case, the optimal loading margins obtained from 2 up to 5 SVCs is always higher than the solution obtained through the sensitivity method (see Table III).
7) The proposed method allows an easy implementation of multiscenario problems, which can be solved in a distributed fashion. This allows considering all different situations at once.
8) The proposed technique is feasible for realistic size networks. Note that CPU time varies fairly linearly with the number of SVCs. Computational times are reasonable considering that a design problem is solved.
9) Even thought the proposed technique requires higher computing time than the sensitivity method, results are considerably better, which makes this approach more appropriate for the allocation of SVCs.

V. CONCLUSION

This paper presents a multistart Benders decomposition technique to maximize the loading margin of a transmission network through the placement of SVCs. A base case and different contingency cases are considered. The proposed algorithm proves to be efficacious in identifying optimal or near-optimal solutions and robust in what refers to computational behavior. The three case studies analyzed provide detailed numerical simulations and prove the good behavior of the proposed technique. The solutions obtained are superior to those obtained using a sensitivity analysis procedure for a number of installed SVCs greater than one.

Future work will focus on modeling other FACTS different than SVCs (e.g., series FACTS devices).

TABLE VIII
40-BUS SYSTEM: TRANSMISSION LINE AND TRANSFORMER THERMAL LIMITS

Line i-j	$\phi_k^{\max}$ (p.u.)
40-38	0.68
38-12	0.28
17-18, 5-6	0.20
11-38, 34-11	0.16
38-14	0.15
14-12	0.13
26-39, 13-12	0.12
5-9	0.11
10-11, 15-16, 11-9	0.10
25-26	0.9
12-15, 24-16, 3-5, 4-5, 8-17, 8-36	0.08
23-17, 12-25	0.07
5-10, 7-17, 16-23	0.05
all other lines	0.04

TABLE IX
THE 40-BUS SYSTEM: GENERATOR REACTIVE POWER LIMITS

Generator bus	$q_{G_i}^{\max}$ (p.u.)	$q_{G_i}^{\min}$ (p.u.)
6	0.0240	-0.0240
13, 24	0.0140	-0.0140
18	0.0275	-0.0275
20, 22	0.0050	-0.0050
39	0.0300	-0.0300
40	0.099	-0.099

APPENDIX

This Appendix provides the limit values used in the 40-bus case study so that the interested reader can readily reproduce paper results. All p.u. values shown in this section are referred to a 100 MVA power base and to transformer voltage ratings. Table VIII provides transmission line and transformer thermal limits, while Table IX provides generator reactive power limits. Maximum and minimum voltage limits are considered to be 1.1 and 0.9 p.u., respectively, for all buses. Finally, SVC maximum and minimum susceptance limits are $b_{C_i}^{\max} = 0.02$ p.u. and $b_{C_i}^{\min} = -0.02$ p.u., respectively.

REFERENCES

[1] E. J. Oliveira, J. W. M. Lima, and K. de Almeida, "Allocation of FACTS devices in hydrothermal systems," *IEEE Trans. Power Syst.*, vol. 15, no. 1, pp. 276–282, Feb. 2000.

[2] T. Orfanogianni and R. Bacher, "Steady-state optimization in power systems with series FACTS devices," *IEEE Trans. Power Syst.*, vol. 18, no. 1, pp. 19–26, Feb. 2003.

[3] N. K. Sharma, A. Ghosh, and R. Varma, "A novel placement strategy for FACTS controllers," *IEEE Trans. Power Del.*, vol. 18, no. 3, pp. 982–987, Jul. 2003.

[4] P. Paterni, S. Vitet, M. Bena, and A. Yokoyama, "Optimal location of phase shifters in the french network by genetic algorithm," *IEEE Trans. Power Syst.*, vol. 14, no. 1, pp. 37–42, Feb. 1999.

[5] S. Gerbex, R. Cherkaoui, and A. J. Germond, "Optimal location of multi-type FACTS devices in a power system by means of genetic algorithms," *IEEE Trans. Power Syst.*, vol. 16, no. 3, pp. 537–544, Aug. 2001.

[6] F. G. M. Lima, F. D. Galiana, I. Kockar, and J. Muñoz, "Phase shifter placement in large-scale systems via mixed integer linear programming," *IEEE Trans. Power Syst.*, vol. 18, no. 3, pp. 1029–1034, Aug. 2003.

[7] E. Vaahedi, Y. Mansour, C. Fuchs, S. Granville, M. D. L. Latore, and H. Hamadanizadeh, "Dynamic security constrained optimal power flow/var planning," *IEEE Trans. Power Syst.*, vol. 16, no. 1, pp. 38–43, Feb. 2001.

[8] N. Yorino, E. E. El-Araby, H. Sasaki, and S. Harada, "A new formulation for FACTS allocation for security enhancement against voltage collapse," *IEEE Trans. Power Syst.*, vol. 18, no. 3, pp. 2–10, Feb. 2003.

[9] C. A. Cañizares, "Voltage Stability Assessment: Concepts, Practices and Tools," in *IEEE/PES Power System Stability Subcommittee, Final Document, Tech. Rep. SP101PSS_2002*, Aug. 2002.

[10] C. A. Cañizares, "Calculating optimal system parameters to maximize the distance to saddle-node bifurcations," *IEEE Trans. Circuits Syst. I*, vol. 45, no. 3, pp. 225–237, Mar. 1998.

[11] W. D. Rosehart, C. A. Cañizares, and V. H. Quintana, "Multi-objective optimal power flows to evaluate voltage security costs in power networks," *IEEE Trans. Power Syst.*, vol. 18, no. 2, pp. 578–587, May 2003.

[12] F. Milano, C. A. Cañizares, and M. Invernizzi, "Multi-objective optimization for pricing system security in electricity markets," *IEEE Trans. Power Syst.*, vol. 18, no. 2, pp. 506–694, May 2003.

[13] K. Xie, Y.-H. Song, J. Stonham, E. Yu, and G. Liu, "Decomposition model and interior point methods for optimal spot pricing of electricity in deregulation environments," *IEEE Trans. Power Syst.*, vol. 15, no. 1, pp. 39–50, Feb. 2000.

[14] A. Conejo, E. Castillo, R. Mínguez, and R. García-Bertrand, *Decomposition Techniques in Mathematical Programming. Engineering and Science Applications*. New York: Springer, 2006.

[15] N. T. Hawkins, "On-line reactive power management in electric power systems," Ph.D. dissertation, Univ. London, London, U.K., 1996.

[16] S. Greene and I. Dobson, *Voltage Collapse Margin Sensitivity Methods Applied to the Power System of Southwest England,* Feb. 1998. [Online]. Available: http://www.pserc.wisc.edu.

[17] A. Brooke, D. Kendrick, A. Meeraus, R. Raman, and R. E. Rosenthal, *GAMS, A User's Guide*. Washington, DC: GAMS Development Corp., 1998.

[18] G. K. Morison, B. Gao, and P. Kundur, "Voltage stability analysis using static and dynamic approaches," *IEEE Trans. Power Syst.*, vol. 8, no. 3, pp. 1159–1171, Aug. 1993.

[19] Univ. Washington Power Systems Test Case Archive. [Online]. Available: http://www.ee.washington.edu/research/pstca.

Roberto Mínguez received the civil engineering degree and the Ph.D. degree in applied mathematics and computer science in September 2000 and June 2003, respectively, from the University of Cantabria, Santander, Spain.

During 2004, he was a Visiting Scholar at Cornell University, Ithaca, NY, under the Fulbright program. He is currently an Assistant Professor of numerical methods in engineering at the University of Castilla-La Mancha, Ciudad Real, Spain. His research interests are reliability engineering, sensitivity analysis, numerical methods, and optimization.

Federico Milano (M'03) received the electrical engineering degree and the Ph.D. degree in electrical engineering from the University of Genoa, Genoa, Italy, in March 1999 and June 2003, respectively.

From September 2001 to December 2002, he worked at the Electrical and Computer Engineering Department of the University of Waterloo, Waterloo, ON, Canada, as a Visiting Scholar. He is currently an Associate Professor of electrical engineering at the University of Castilla-La Mancha, Ciudad Real, Spain.

His research interests are voltage stability, electricity markets, and computer-based power system modeling.

Rafael Zárate-Miñano (S'05) received the electrical engineering degree in April 2005 from the Universidad of Castilla-La Mancha, Ciudad Real, Spain, where he is currently pursuing the Ph.D. degree.

His research interests include voltage stability, electricity markets, sensitivity analysis, optimization, and numerical methods.

Antonio J. Conejo (F'04) received the M.S. degree from the Massachusetts Institute of Technology, Cambridge, in 1987 and the Ph.D. degree from the Royal Institute of Technology, Stockholm, Sweden, in 1990.

He is currently a full Professor at the University of Castilla-La Mancha, Ciudad Real, Spain. His research interests include control, operations, planning, and economics of electric energy systems, as well as statistics and optimization theory and its applications.